Analytical expressions pertaining to the concentration of catechol, o-quinone and current at PPO-modified microcylinder biosensor for diffusion-kinetic model

ARTICLE *in* JOURNAL OF ELECTROANALYTICAL CHEMISTRY · SEPTEMBER 2011

Impact Factor: 2.73 · DOI: 10.1016/j.jelechem.2011.06.033

2 AUTHORS, INCLUDING:

Lakshmanan Rajendran
Sethu Institute of Technology
135 PUBLICATIONS **409** CITATIONS

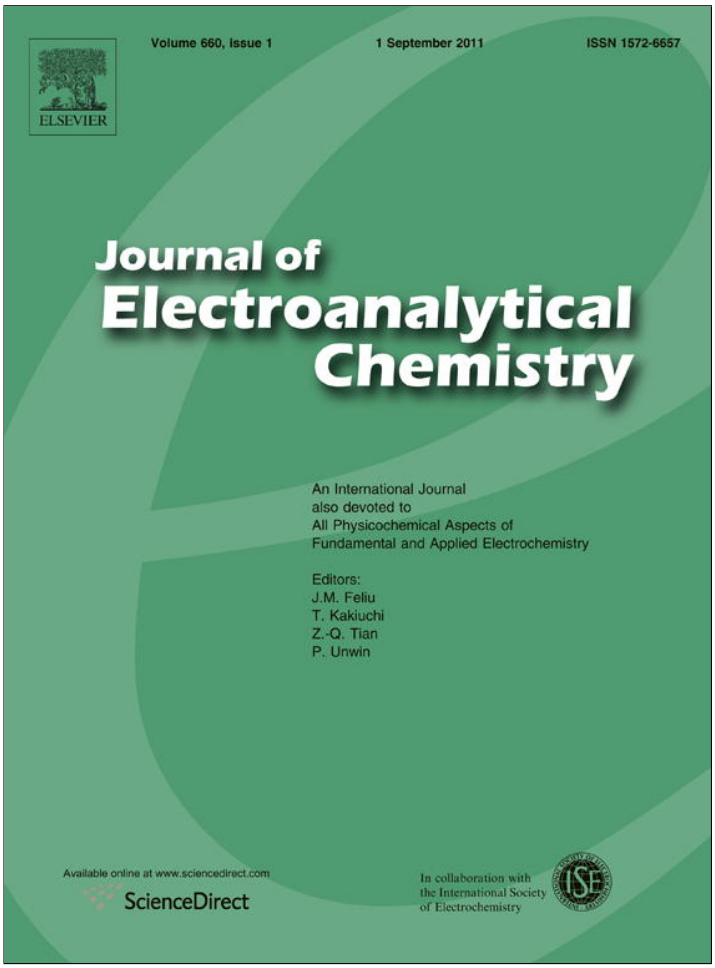

Journal of Electroanalytical Chemistry 660 (2011) 200–208

Contents lists available at ScienceDirect

Journal of Electroanalytical Chemistry

journal homepage: www.elsevier.com/locate/jelechem

Analytical expressions pertaining to the concentration of catechol, *o*-quinone and current at PPO-modified microcylinder biosensor for diffusion-kinetic model

A. Eswari, L. Rajendran *

Department of Mathematics, The Madura College, Madurai 625011, Tamil Nadu, India

ARTICLE INFO

Article history:
Received 7 April 2011
Received in revised form 24 June 2011
Accepted 29 June 2011
Available online 8 July 2011

Keywords:
Non-linear reaction/diffusion equation
Biosensors
Michaelis–Menten kinetics
Polymer-modified microcylinder electrode
Mathematical modeling

ABSTRACT

A theoretical model for electroenzymatic process of a modified microcylinder electrode in which polyphenol oxidase occurs for all values of the concentration of catechol and *o*-quinone is presented. The model is based on system of reaction–diffusion equations containing a non-linear term related to Michaelis–Menten kinetics of the enzymatic reaction. In this paper, we implement a new analytical technique (He's variational iteration method) is used to solve the system of non-linear differential equations that describe the diffusion coupled with a Michaelis–Menten kinetics law. Herein, we report the closed form of an analytical expressions pertaining to the concentration of catechol and *o*-quinone and corresponding current in terms of dimensionless reaction–diffusion parameters γ_E, γ_S, α, $r_1/r_0(=\alpha_1)$, enzyme kinetics (χr_0) and Michaelis–Menten constant (K_M). A simple relation between the concentration of catechol and *o*-quinone also obtained. A good agreement with available limiting case results is noticed. The obtained results are valid for the whole solution domain.

1. Introduction

The main interest of PPO system resides in the fact that both catechol substrate (S) and orthoquinone product (P) of the enzymatic reaction are electroactive. S and P can thus be independently monitored at the electrode surface by applying a sufficiently cathodic potential (P monitoring) or anodic potential (S monitoring) and recording the resulting current [1]. In a recent series of papers [1–3], Labbe presented a theoretical analysis of the transport and kinetics of substrate and product in an immobilized enzyme layer involving an electrochemical substrate-recycling scheme. Labbe analysis was conducted using catechol–polyphenol oxidase (PPO) as a prototype electroenzymatic model system [4]. The layer-by-layer technique introduced by Decher [5] suffices these requirements for immobilization in various matrices [6–9]. This method is composed of building-up a positively charged polyelectrolyte and a negatively charged layer alternately on a substrate derivatized with a stable surface charge excess [9–12]. The immobilization has been ascribed to the electrostatic interaction between neighboring layers [13–16]. Rijiravanich et al. [17] report the construction and kinetic analysis of cylindrical microelectrode sensors, consisting of single carbon fibres modified by PPO immobilized on latex (denoted Ty-La) by an LbL process. To characterize the sensors, Rijiravanich and co-workers [17] have derived a general diffusion-kinetic model of the steady state current at PPO-modified microcylinders.

Recently Rijiravanich et al. [17] obtained the steady state concentration profile of *o*-quinone and dimensionless sensor response *j* for the limiting case of low substrate concentrations. To the best of our knowledge, no rigorous analytical solutions for the steady-state concentration of catechol and *o*-quinone and the current for microcylinder biosensors for all values of the parameters have been published. In this paper, we have derived a simple analytical expression of the concentration of catechol and *o*-quinone and the current for all values of substrate concentration using variational iteration method.

2. Mathematical formulation of the problem and analysis

The electrode is used in a stirred solution containing an excess of supporting electrolyte. The enzyme and electrode reaction are [17]:

$$O_2 + 2\text{catechol} \rightarrow 2o\text{-quinone} + 2H_2O \quad (1)$$

$$o\text{-quinone} + 2H^+ + 2e^- \rightarrow \text{catechol} \quad (2)$$

Hence the catechol/*o*-quinone conversion forms an amplification cycle within the enzyme film. While it is possible in principle to solve for either phenol or catechol as substrate, solving for catechol is simpler, since it involves only one enzymic conversion. The actual mechanism of that conversion is complex, and involves three different states, oxy, met, deoxy [18] which is represented in [17]. The process may be represented by Michaelis–Menten kinetics, i.e.

* Corresponding author. Tel.: +91 9442228951; fax: +91 0452 2675238.
E-mail address: raj_sms@rediffmail.com (L. Rajendran).

1572-6657/$ - see front matter © 2011 Elsevier B.V. All rights reserved.
doi:10.1016/j.jelechem.2011.06.033

$$k_{cat} = k_1 c_{O_2} \quad \text{and} \quad K_M = \frac{k_1(k_2+k_3)c_{O_2}}{k_2 k_3} \tag{3}$$

The mass balance for catechol c_C can be written in cylindrical coordinates:

$$\frac{D_C}{r}\frac{d}{dr}\left(r\frac{dc_C}{dr}\right) - \frac{k_{cat}c_E c_C}{c_C + K_M} = 0 \tag{4}$$

where c_C is the concentration profile of catechol, c_E is the concentration profile of enzyme, D_C and D_Q are its diffusion coefficients, and K_M is the Michaelis constant and c_Q is the concentration profile of quinone. Then the equation of continuum for quinone is generally expressed in the steady-state by

$$\frac{D_Q}{r}\frac{d}{dr}\left(r\frac{dc_Q}{dr}\right) + \frac{k_{cat}c_E c_C}{c_C + K_M} = 0 \tag{5}$$

At the electrode surface (r_0) and at the film surface (r_1) the boundary conditions are [17]

$$\begin{aligned} r = r_0 &: c_C = c_C^*, \quad c_Q = 0 \\ r = r_1 &: c_C = c_C^*, \quad c_Q = 0 \end{aligned} \tag{6}$$

where c_C^* is the bulk concentration of catechol scaled by the partition coefficient of the enzyme film. Adding Eqs. (4) and (5) and integrating successful with boundary condition (6), we get

$$\frac{c_C(r)}{c_C^*} + \frac{D_Q c_Q(r)}{D_C c_C^*} = 1 \tag{7}$$

The steady-state current can be given as [17]:

$$\frac{I}{nF} = 2\pi L r_0 D_Q (dc_Q/dr)_{r=r_0} \tag{8}$$

We introduce the following set of dimensionless variables:

$$\begin{aligned} &C = \frac{c_C}{c_C^*}, \quad Q = \frac{c_Q}{c_C^*}, \quad R = \frac{r}{r_0}, \quad \alpha = \frac{c_C^*}{K_M}, \\ &\gamma_E = \frac{k_{cat}c_E r_0^2}{D_C K_M}, \quad \gamma_S = \frac{k_{cat}c_E r_0^2}{D_Q K_M}, \quad \frac{D_Q}{D_C} = \frac{\gamma_E}{\gamma_S} \end{aligned} \tag{9}$$

where C and Q are the dimensionless concentration of the catechol and o-quinone. R is the dimensionless distance parameter. γ_E,γ_S and α are the dimensionless reaction–diffusion parameters and saturation parameter.

$$\frac{d^2C}{dR^2} + \frac{1}{R}\frac{dC}{dR} - \frac{\gamma_E C}{1+\alpha C} = 0 \tag{10}$$

$$\frac{d^2Q}{dR^2} + \frac{1}{R}\frac{dQ}{dR} + \frac{\gamma_S C}{1+\alpha C} = 0 \tag{11}$$

The boundary conditions are represented as follows:

$$C = 1, \quad Q = 0 \quad \text{when } R = 1 \tag{12}$$

$$C = 1, \quad Q = 0 \quad \text{when } R = r_1/r_0 \tag{13}$$

The dimensionless current at the microcylinder electrode can be given as follows:

$$\psi = I/nFLD_Q c_C^* = 2\pi(dQ/dR)_{R=1} \tag{14}$$

Using variational iteration method [19–26] (see Appendix A), we can obtain the following solutions to Eqs. (10) and (11):

$$\begin{aligned} C(R) = \big[&1 - 3a - 4a\alpha - 2.667a^2\alpha - \gamma_E - 0.667a\gamma_E \\ &+(4a + 4a\alpha + 4a^2\alpha + \gamma_E + \gamma_E a)R - aR^2 - 1.333a^2\alpha R^3 \\ &-0.333\gamma_E a R^3\big] \end{aligned} \tag{15}$$

$$\begin{aligned} Q(R) = \frac{\gamma_S}{\gamma_E}\big[&3a + 4a\alpha + 2.667a^2\alpha + \gamma_E + 0.667\gamma_E a \\ &+(-4a - 4\alpha a - \gamma_E - \gamma_E a - 4\alpha a^2)R + aR^2 + 1.333a^2\alpha R^3 \\ &+0.333\gamma_E a R^3\big] \end{aligned} \tag{16}$$

where

$$\begin{aligned} a = 0.5\Big(&-\gamma_E(r_1/r_0)^2 - 3r_1/r_0 - \gamma_E(r_1/r_0) + 9 + 12\alpha + 2\gamma_E - \sqrt{A}\Big) \\ &/(4\alpha(r_1/r_0) - 8\alpha + 4\alpha(r_1/r_0)^2) \end{aligned} \tag{16a}$$

and

$$\begin{aligned} A = {} & 81 + 216\alpha + 36\gamma_E - 12(r_1/r_0)^2\gamma_E - 30\gamma_E(r_1/r_0) \\ & - 54(r_1/r_0) + 24(r_1/r_0)^2\gamma_E\alpha - 48\gamma_E\alpha + 4\gamma_E^2 - 3\gamma_E^2(r_1/r_0)^2 \\ & - 4\gamma_E^2(r_1/r_0) + 24\gamma_E\alpha(r_1/r_0) - 72\alpha(r_1/r_0) + 6\gamma_E(r_1/r_0)^3 \\ & + 9(r_1/r_0)^2 + (r_1/r_0)^4\gamma_E^2 + 2\gamma_E^2(r_1/r_0)^3 + 144\alpha^2 \end{aligned} \tag{16b}$$

Eqs. (15) and (16) satisfies the boundary conditions (12) and (13). These equations represent the new and simple analytical expression of the concentration of catechol and o-quinone for all possible values of the parameters γ_E, γ_S, α and r_1/r_0. Eqs. (15) and (16) also satisfy the relation $C(R) + (\gamma_E/\gamma_S)Q(R) = 1$. From Eqs. (14) and (16), we can obtain the dimensionless current, which is as follows:

$$\psi = I/nFLD_Q c_C^* = 2\pi(\gamma_S/\gamma_E)[-2a - 4a\alpha - \gamma_E] \tag{17}$$

Table 1
Values of p and q which fit Eq. (31) to Eq. (30) with <5% error [17].

x	p	q
9.0–7.0	1.00	1.01
6.0–4.0	1.03	1.05
3.0	1.04	1.10
2.0	1.02	1.14[a]/1.25[b]

[a] Valid for $\alpha_1 \leqslant 2.0$.
[b] Valid for $\alpha_1 > 2.0$.

Table 2
Comparison of dimensionless sensor response j for various values of χr_0 using Eqs. (28) and (33) when thickness of the film ($\alpha_1 = r_1/r_0 = 5$).

$x(=\chi r_0)$	$\alpha_1 = r_1/r_0$	p	q	Eq. (33) [17]	Eq. (28) This work	Error (%)
9.0	5	1	1.01	57.7756	57.7755	0.0002
8.5	5	1	1.01	54.5346	54.543	0.01540
8	5	1	1.01	51.2956	51.2952	0.0008
7.5	5	1	1.01	48.0586	48.0577	0.0019
7	5	1	1.01	44.8237	44.7790	0.0998
5.5	5	1.03	1.05	37.6132	37.5890	0.0644
5	5	1.03	1.05	34.0312	34.0112	0.0588
4.5	5	1.03	1.05	30.4672	29.9984	1.5628
4	5	1.03	1.05	26.9229	25.9457	3.7663
3	5	1.04	1.10	21.0276	20.9874	0.1915
2	5	1.02	1.25	14.9284	14.9269	0.0100
Average % deviation						0.5247

Table 3
Comparison of dimensionless sensor response j for various values of χr_0 using Eqs. (28) and (33) when thickness of the film ($\alpha_1 = r_1/r_0 = 1.5$).

$x(=\chi r_0)$	$\alpha_1 = r_1/r_0$	p	q	Eq. (33) [17]	Eq. (28) This work	Error (%)
9.0	1.5	1	1.01	56.5061	56.5060	0.0002
8.5	1.5	1	1.01	53.0008	53.0114	0.0199
8	1.5	1	1.01	49.4504	49.4523	0.0038
7.5	1.5	1	1.01	45.8501	45.8726	0.0490
7	1.5	1	1.01	42.1960	42.1875	0.0201
5.5	1.5	1.03	1.05	32.8466	32.9980	0.4588
5	1.5	1.03	1.05	28.6172	27.6047	3.6679
4.5	1.5	1.03	1.05	24.4092	23.9984	1.7118
4	1.5	1.03	1.05	20.2679	20.4321	0.8036
3	1.5	1.04	1.10	13.0951	13.1543	0.4500
2	1.5	1.02	1.14	6.3205	6.3211	0.0095
Average % deviation						0.6541

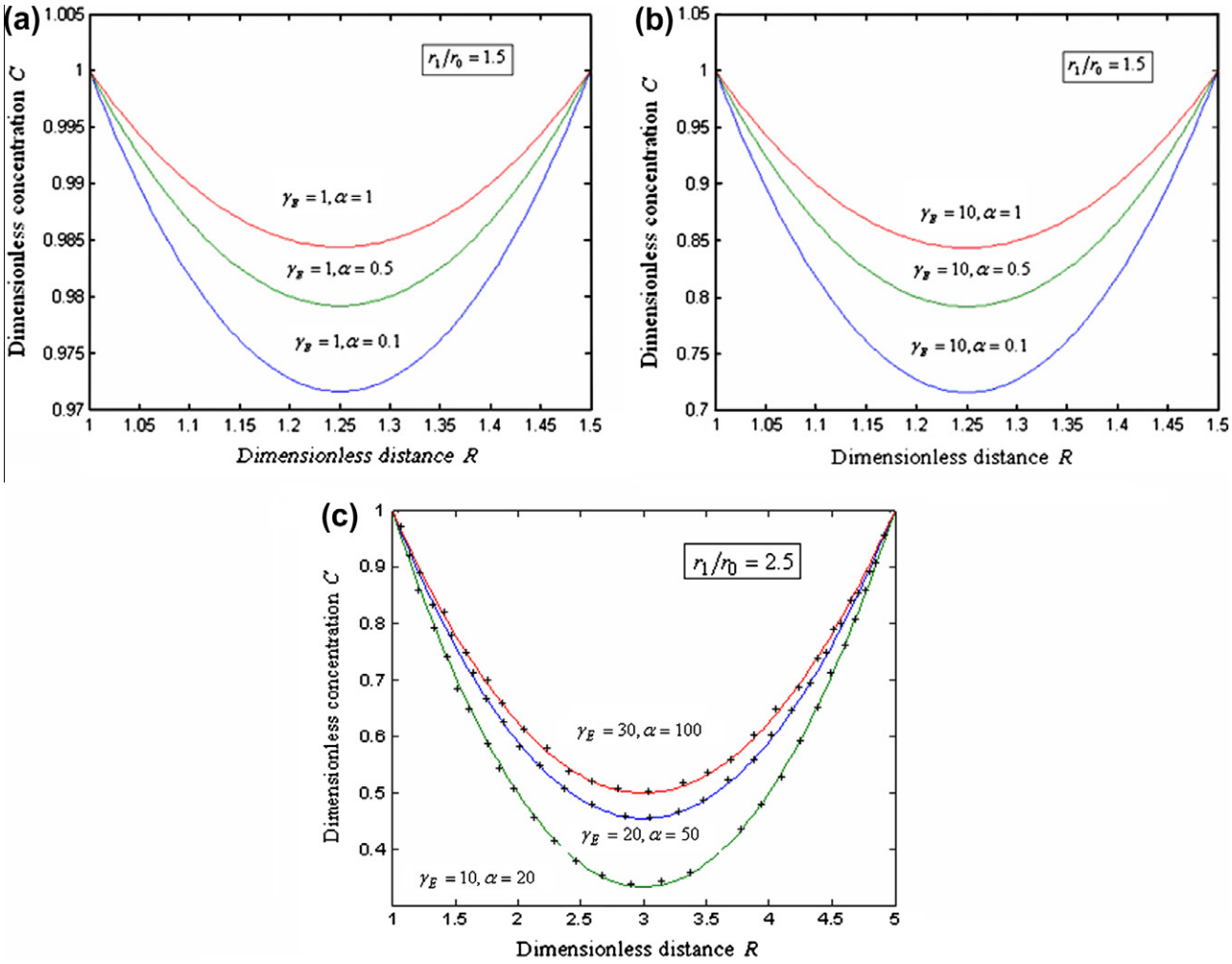

Fig. 1. Typical normalized steady-state concentration profile of catechol $C(R)$ plotted from Eq. (15) for different values of parameters γ_E and α when $r_1/r_0 = 1.5, 2.5$. Symbols: (__) Eq. (15) and (+++) Eq. (20) (Zero order catalytic kinetic).

Eq. (17) represents the new and closed form of an analytical expression for the current for all possible values of parameters.

3. Limiting case result

(i) *Saturated (Zero order) catalytic kinetics*In this case, the catechol concentration C is greater than Michaelis constant K_M. When $\alpha C \gg 1$, Eqs. (10) and (11) reduce to the following forms:

$$\frac{d^2C}{dR^2} + \frac{1}{R}\frac{dC}{dR} - \frac{\gamma_E}{\alpha} = 0 \tag{18}$$

$$\frac{d^2Q}{dR^2} + \frac{1}{R}\frac{dQ}{dR} + \frac{\gamma_S}{\alpha} = 0 \tag{19}$$

By solving Eqs. (18) and (19), we can obtain the concentration of catechol C and *o*-quinone Q as follows:

$$C(R) = \frac{1}{4\alpha}\left[\gamma_E R^2 - \frac{\gamma_E[(r_1/r_0)^2 - 1]\ln(R)}{\ln(r_1/r_0)} - \gamma_E + 4\alpha\right] \tag{20}$$

$$Q(R) = \frac{1}{4\alpha}\left[-\gamma_S R^2 + \frac{\gamma_S[(r_1/r_0)^2 - 1]\ln(R)}{\ln(r_1/r_0)} + \gamma_S\right] \tag{21}$$

The normalized current is given by

$$\psi = I/nFLD_Q c_C^* = \frac{\pi\gamma_S}{2\alpha\ln(r_1/r_0)}[(r_1/r_0)^2 - 1 - 2\ln(r_1/r_0)] \tag{22}$$

Eqs. (20)–(22) denote the new closed expression of dimensionless concentrations of C, Q and dimensionless current ψ for all values of the parameters γ_E, γ_S, α and r_1/r_0.

(ii) *Unsaturated (first order) catalytic kinetics*In this case, the catechol concentration c_C is less than Michaelis constant K_M. Now Eqs. (5) and (6) reduce to the following forms:

$$\frac{D_C}{r}\frac{d}{dr}\left(r\frac{dc_C}{dr}\right) - \frac{k_{cat}c_E c_C}{K_M} = 0 \tag{23}$$

$$\frac{D_Q}{r}\frac{d}{dr}\left(r\frac{dc_Q}{dr}\right) + \frac{k_{cat}c_E c_C}{K_M} = 0 \tag{24}$$

By solving Eq. (23) using the boundary condition (Eq. (6)), the concentration of catechol c_C can be obtained in the form of modified Bessel functions of zeroth order $I_0(\chi r)$ and $K_0(\chi r)$.

$$c_C(r)/c_C^* = \left[\frac{I_0(\chi r)[K_0(\chi r_0) - K_0(\chi r_1)] + K_0(\chi r)[I_0(\chi r_1) - I_0(\chi r_0)]}{K_0(\chi r_0)I_0(\chi r_1) - K_0(\chi r_1)I_0(\chi r_0)}\right] \tag{25}$$

where

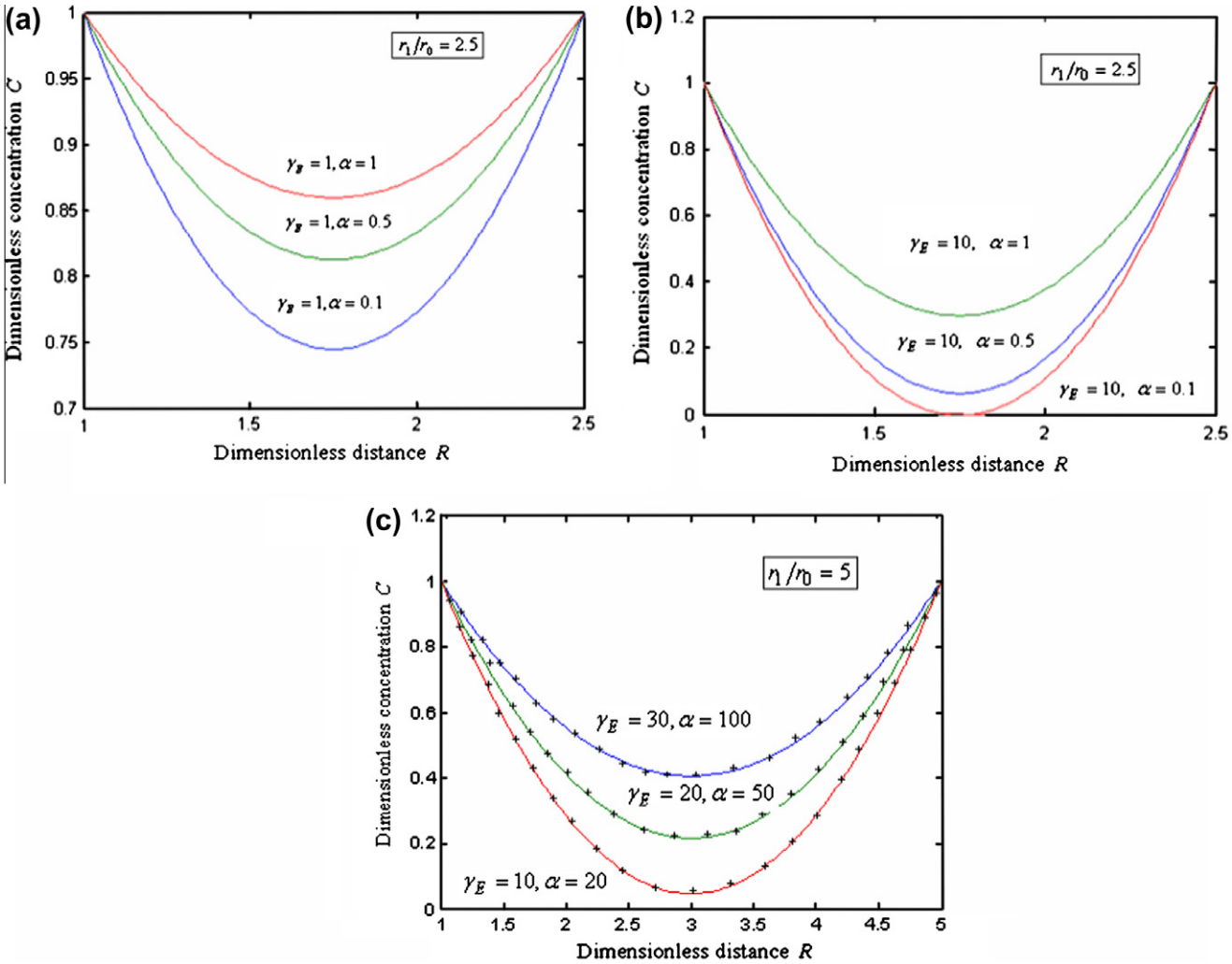

Fig. 2. Typical normalized steady-state concentration profile of catechol $C(R)$ plotted from Eq. (15) for different values of parameters γ_E and α when $r_1/r_0 = 2.5,5$. Symbols: (—) Eq. (15) and (+++) Eq. (20) (Zero order catalytic kinetic).

$$\chi^2 = k_{cat} c_E / D_C K_M \tag{26}$$

Inserting Eq. (25) into Eq. (7), we can obtain the concentration c_Q

$$\frac{D_Q c_Q(r)}{D_C c_C^*} = 1 - \left[\frac{I_0(\chi r)[K_0(\chi r_0) - K_0(\chi r_1)] + K_0(\chi r)[I_0(\chi r_1) - I_0(\chi r_0)]}{K_0(\chi r_0) I_0(\chi r_1) - K_0(\chi r_1) I_0(\chi r_0)}\right] \tag{27}$$

The sensor response j in terms of modified Bessel function of zeroth order can be obtained as follows:

$$j = \frac{I}{nFLD_C c_C^*} = \frac{2\pi\chi r_0}{[K_0(\chi r_0) I_0(\chi r_1) - K_0(\chi r_1) I_0(\chi r_0)]} \{K_1(\chi r_0)[I_0(\chi r_1) - I_0(\chi r_0)] - I_1(\chi r_0)[K_0(\chi r_0) - K_0(\chi r_1)]\} \tag{28}$$

When the enzyme kinetic term is very small (χr_0 and $\chi r_1 \to 0$, i.e., it is purely diffusion limited) Eq. (28) becomes

$$j = \frac{I}{nFLD_C c_C^*} \approx \pi(\chi r_0)^2 \tag{29}$$

When the enzyme kinetic term is very large (χr_0 and $\chi r_1 \to \infty$) Eq. (28) becomes

$$j = \frac{I}{nFLD_C c_C^*} \approx 2\pi \left[\frac{(\chi r_0)^{3/2}\{\sqrt{\chi r_0}\exp(\chi r_1 - \chi r_0) - \sqrt{\chi r_1}\} - (\chi r_0)\sqrt{\chi r_1}\{\sqrt{\chi r_0} - \sqrt{\chi r_1}\exp(\chi r_0 - \chi r_1)\}}{(\chi r_0)\exp(\chi r_1 - \chi r_0) - (\chi r_1)\exp(\chi r_0 - \chi r_1)}\right] \tag{30}$$

The above limiting case result is used to find the diffusion coefficient. Recently Rijiravanich et al. [17] have discussed about the concentration c_Q and the sensor response j for various values of the parameters χr_0 and r_1/r_0.

4. Comparison with limiting case work of Rijiravanich et al. [17]

Recently, Rijiravanich et al. [17] have derived the analytical expression of the steady-state concentration c_Q (Eq. (31)) and sensor response j (Eqs. (31) and (32)) in integral form for the limiting case $c_C < K_M$.

$$\frac{D_Q c_Q(r)}{D_C c_C^*} = g\chi\left\{-f\int_{r_0}^{r} I_1(\chi r)dr + \int_{r_0}^{r} K_1(\chi r)dr + \frac{\ln(r/r_0)}{\ln(r_1/r_0)} \times \left[f\int_{r_0}^{r_1} I_1(\chi r)dr - \int_{r_0}^{r_1} K_1(\chi r)dr\right]\right\} \tag{31}$$

$$j = \frac{I}{nFLD_C c_C^*} = 2\pi\chi g \mathrm{X}\left\{r_0[-fI_1(\chi r_0) + K_1(\chi r_0)] + \frac{1}{\ln(r_1/r_0)}\left[f\int_{r_0}^{r_1} I_1(\chi r)dr - \int_{r_0}^{r_1} K_1(\chi r)dr\right]\right\} \tag{32}$$

where $g = 1/[fI_0(\chi r_0) + K_0(\chi r_0)]$, $f = [K_0(\chi r_0) - K_0(\chi r_1)]/[I_0(\chi r_1) - I_0(\chi r_0)]$. Rijiravanich et al. [17] obtained the empirical expression of the current

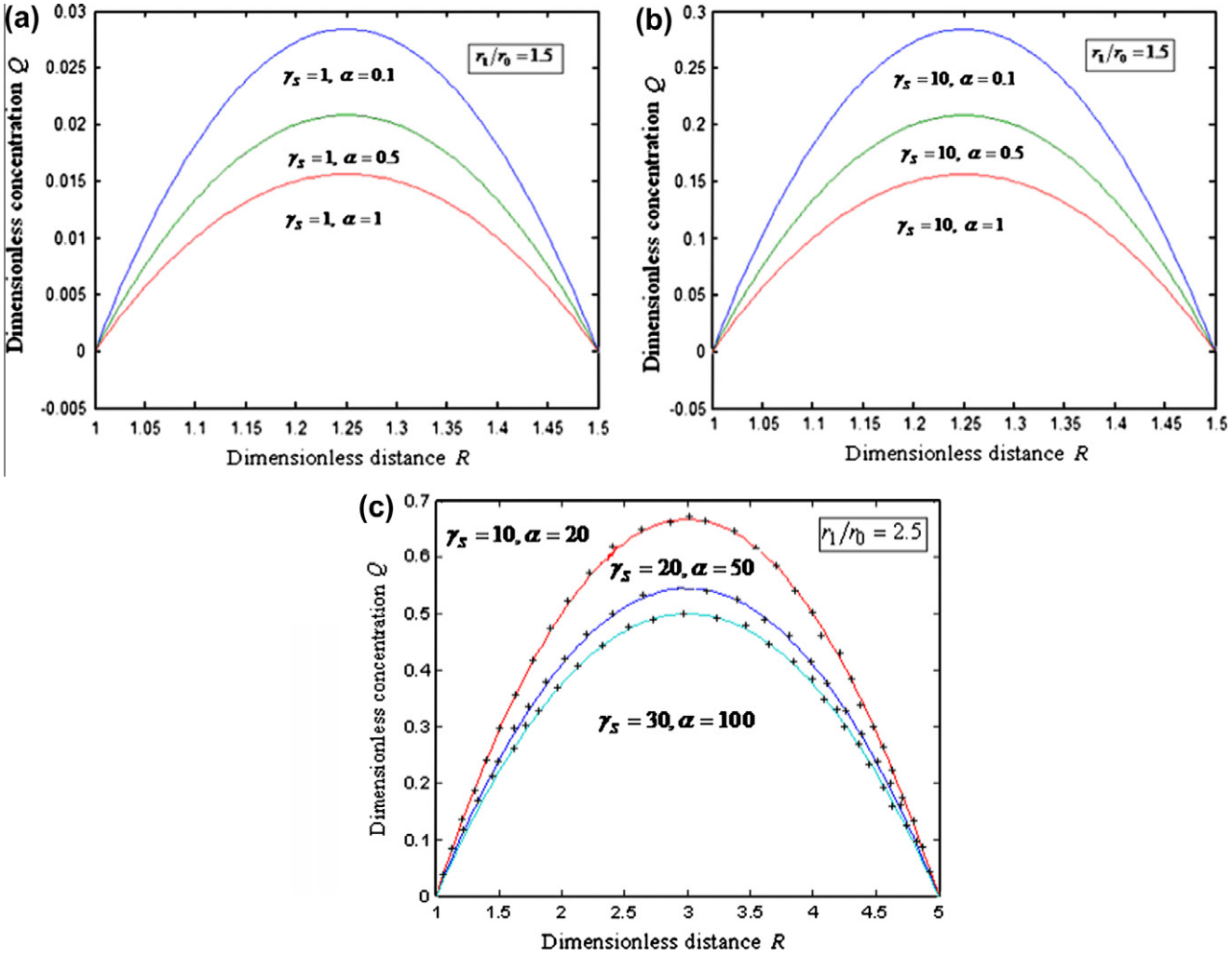

Fig. 3. Typical normalized steady-state concentration profile of o – quinone $Q(R)$ plotted from Eq. (16) for different values of parameters γ_S and α and the fixed value of $\gamma_E = 0.0001$ when $r_1/r_0 = 1.5, 2.5$. Symbols: (__) Eq. (16) and (+++) Eq. (21) (Zero order catalytic kinetic).

$$j = 2\pi x^q \tanh[(x/2)(\alpha_1 - 1)]^p \quad (33)$$

where p and q are empirical constants and $\alpha_1 = r_1/r_0$. The value of p and q are given for various values of $x(=\chi r_0)$ in the Tables 1–3. This empirical expression is compared our simple closed analytical expression Eq. (28), in Tables 2 and 3. The average relative difference between our Eq. (28) and the empirical expression Eq. (33) is 0.65% when $\alpha_1 = 1.5$ and 0.52% when $\alpha_1 = 5$.

5. Discussion

Eqs. (15) and (16) represent the new approximate analytical expression of concentration of catechol and o-quinone for all values of the parameters γ_S, γ_E, r_1/r_0 and α. It satisfies the boundary conditions Eqs. (12) and (13). In Figs. 1a, b, 2a and b, we present the series of the normalized concentration profiles for a catechol $C(R)$ as a function of reaction–diffusion parameters γ_S, γ_E, film thickness r_1/r_0 and saturation parameter α. From the figures, it is inferred that the catechol concentration $C(R)$ is in the form of parabola with $R = 1.25, 1.75, 3$ as the axis of parabola. The value of catechol concentration C is approximately equal to 1 when $R = 1$ and $R = r_1/r_0$ for all values of α and γ_E. When saturation parameter (α) is large (or) reaction–diffusion parameter (γ_E) is very small, the concentration of catechol = 1 for all values of film thickness r_1/r_0. Quinone concentration $Q(R)$ is plotted in Figs. 3a, b, 4a and b for various values of α and γ_S. From these figures, it is concluding that, the value of concentration Q increases when γ_S increases and α decreases. Whereas the concentration of o-quinone is zero when the reaction–diffusion parameter (γ_S) is very small (or) saturated parameter (α) is large for all values of r_1/r_0. In Figs. 1c–4c our analytical expression of concentration of catechol $C(R)$ (Eq. (15)) and concentration of o-quinone $Q(R)$ (Eq. (16)) are compared with the limiting case results (saturated (zero order) catalytic kinetics (Eqs. (20) and (21))). A satisfactory agreement is noted.

From Figs. 1 and 2, we can observed that as the enzyme activity increases, the concentration of catechol falls at the centre of the film, but remains high at the film/solution interface, due to diffusion from bulk and at the electrode/film interface due to generation at the electrode. In complete reverse process occurs for the concentration of o-quinone (refer Figs. 3 and 4). The dimensionless current ψ versus r_1/r_0 using Eq. (17) is plotted in Fig. 5a–c. In Fig. 5c our steady-state analytical expression of current (Eq. (17)) is compared with saturated result (Eq. (22)). The film thickness and enzyme kinetics affect the linearity is shown by Eq. (17). The value of current ψ increases when thickness of the film r_1/r_0 increases for all values of α and γ_S. Also the current increases when γ_S increases (or) α decreases.

Limiting cases

Fig. 6a and b represents the concentration of o-quinone versus $(r - r_0)/(r_1 - r_0)$ for various values of enzyme kinetic. The value of

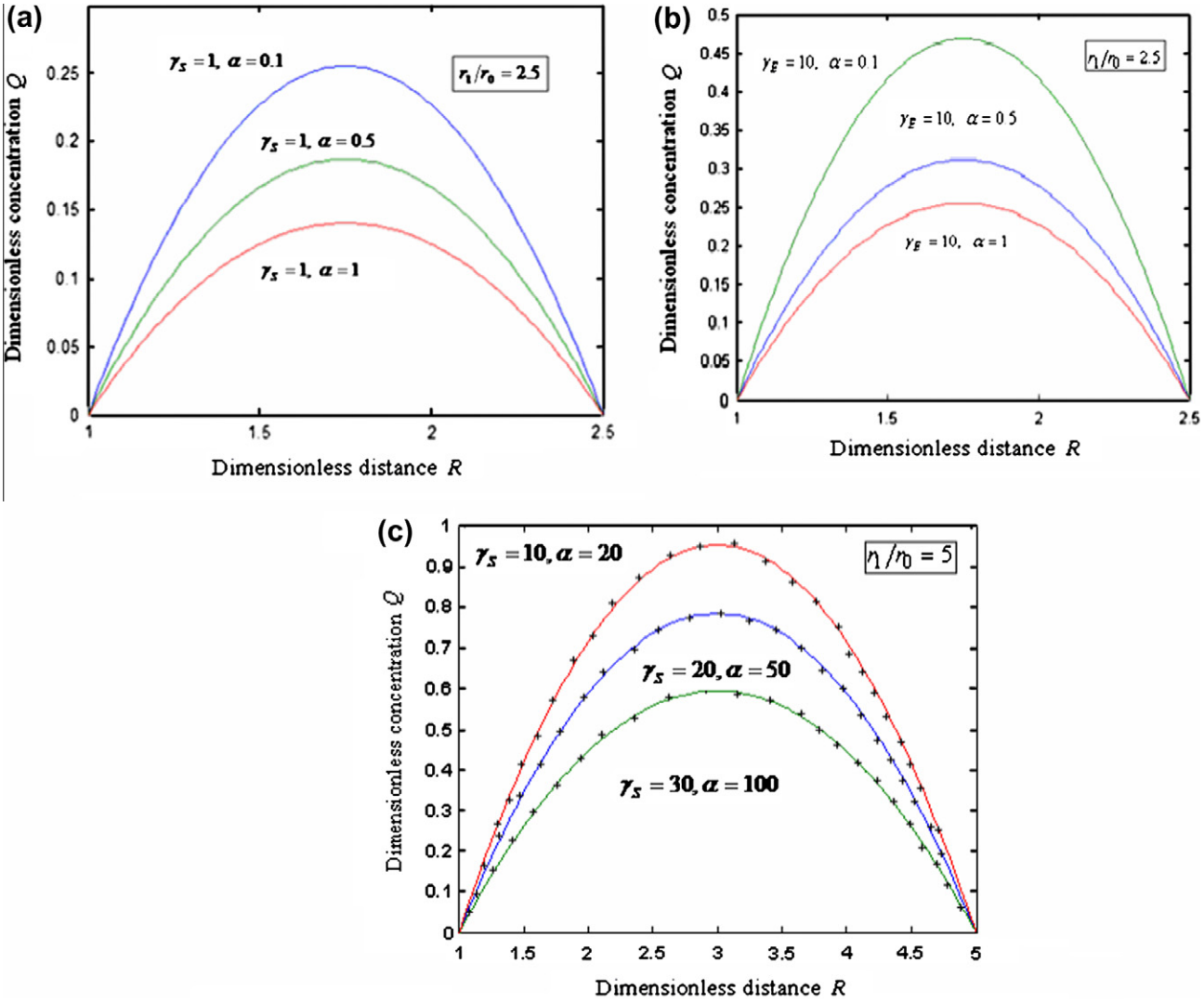

Fig. 4. Typical normalized steady-state concentration profile of o – quinone $Q(R)$ plotted from Eq. (16) for different values of parameters γ_S and α and the fixed value of $\gamma_E = 0.0001$when $r_1/r_0 = 2.5, 5$. Symbols: (__) Eq. (16) and (+++) Eq. (21) (Zero order catalytic kinetic).

concentration reaches the maximum value at $(r - r_0)/(r_1 - r_0) = 0.5$ for all values of χr_0. The concentration of $D_Q c_Q(r)/D_C c_C^*$ is like a normal distributions. The value of $D_Q c_Q(r)/D_C c_C^*$ increases when χr_0 increases. From Fig. 6a and b it can be observed that at high values of $\chi r_0 (\chi r_0 \geqslant 50)$ the normalized concentration of o-quinone through the central region of the film will approach the value 1. Fig. 7 represents the dimensionless sensor response j, as a function of r_1/r_0 for different enzyme reaction/substrate diffusion ratios χr_0. The value of current increases abruptly and reaches the constant value when χr_0 increases. The sensor response j first increases when the thickness of the enzyme layer increases and then to become the thickness independent (or) constant value.

6. Conclusions

In this paper, the coupled time-independent non-linear reaction/diffusion equations have been formulated and solved analytically using variational iteration method. We have presented a diffusion-kinetic model of the steady-state concentration and current and sensor response at PPO-modified microcylinder biosensors. We have presented a simple and closed form of an analytical expressions corresponding to the concentration of the catechol and concentration of the o-quinone in terms of the parameters γ_E, γ_S, α and r_1/r_0 and χr_0.

Previously PPO models (both planar and cylindrical) have only considered the first order kinetics of the enzyme and therefore could only be applied to the sensor's linear range. However, in this paper, calibration curves of many of the catechol/phenol biosensors contain significant non-linear contributions are reported. Also, the length of the linear range is an important analytical parameter. In developing a sensor, experimental scientists would like this range to cover all concentrations expected in real samples, as this makes calibration of the sensor in the field much easier. Furthermore, on the basis of the outcome of this work, it is possible to calculate the approximate amounts of the concentration of the catechol and concentration of the o-quinone, and the sensor response and current corresponding to a nonlinear Michaelis–Menten kinetic scheme. In addition, the transport and kinetics are quantified in terms of kinetic parameter, film thickness and Michaelis–Menten constant.

Acknowledgements

This work was supported by the Department of Science and Technology (DST), Government of India. The authors are thankful to Dr.R.Nagarathinam, The Prinicipal, The Madura College, Madurai and Mr. M.S. Meenakshisundaram, The Secretary, Madura College Board, Madurai for their encouragement. We thank the reviewers

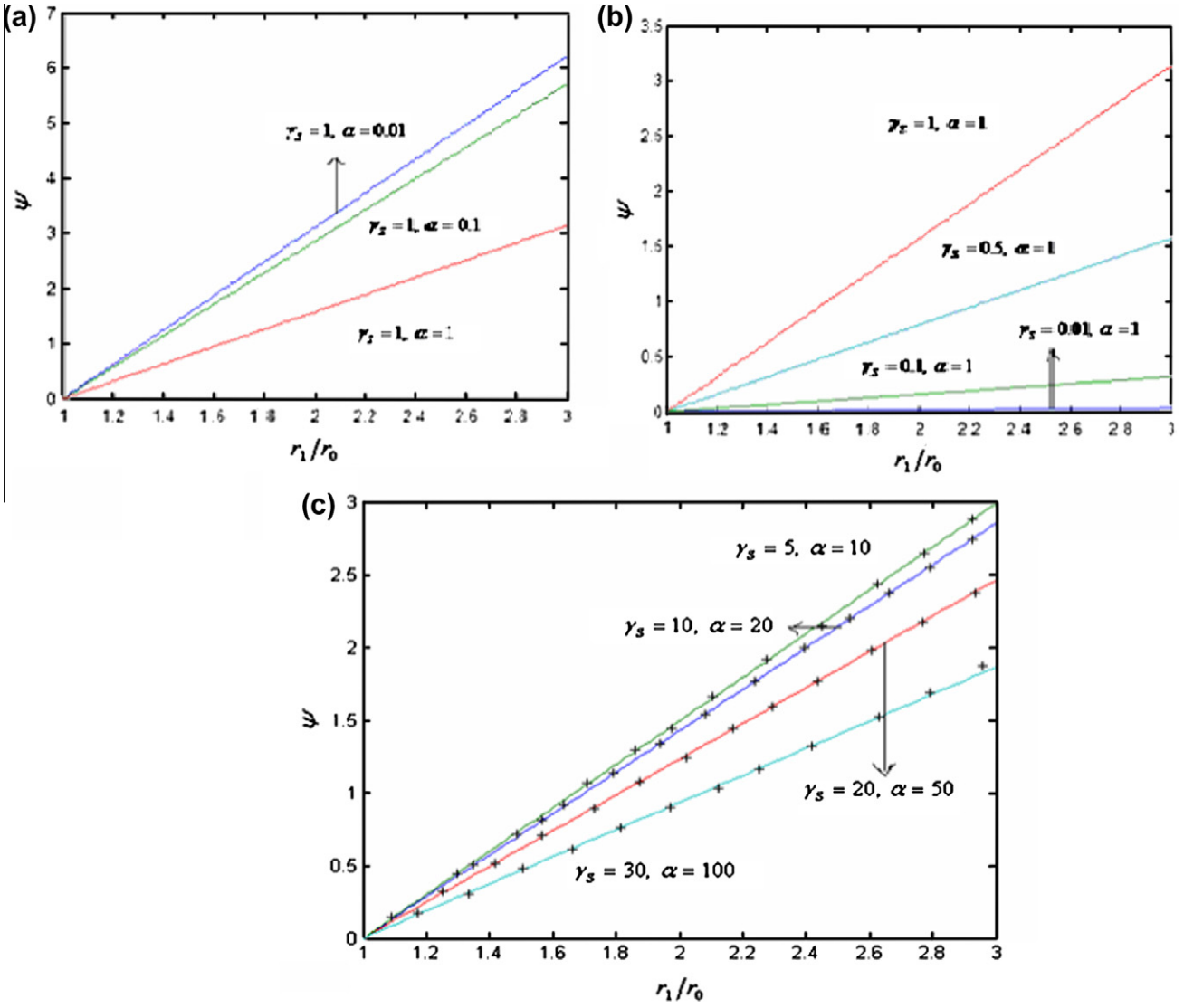

Fig. 5. Plot of dimensionless current ψ versus r_1/r_0 for various values of γ_S and α and the fixed value of $\gamma_E = 0.0001$. Current is calculated using Eq. (17). Symbols: (__) Eq. (17) and (+++) Eq. (22) (Zero order catalytic kinetic).

for their valuable comments to improve the quality of the manuscript.

Appendix A

In this appendix, we derive the general solution of non-linear reaction Eq. (10) using He's variational iteration method. To illustrate the basic concepts of variational iteration method (VIM), we consider the following non-linear partial differential equation [19–23]

$$L[C(R)] + N[C(R)] = g(R) \tag{A1}$$

where L is a linear operator, N is a non-linear operator, and $g(R)$ is a given continuous function. According to the variational iteration method, we can construct a correct functional as follows [22]:

$$C_{n+1}(R) = C_n(R) + \int_1^R \lambda[L[C_n(\tau)] + N[\widetilde{C}_n(\tau)] - g(\tau)]d\tau \tag{A2}$$

where λ is a general Lagrange multiplier which can be identified optimally via variational theory, C_n is the nth approximate solution, and $\widetilde{C}_n$ denotes a restricted variation, i.e., $\delta\widetilde{C}_n = 0$. In this method, a trial function (an initial solution) is chosen which satisfies given boundary conditions. Using the above variational iteration method we can write the correction functional of Eq. (10) as follows:

$$C_{n+1}(R) = C_n(R) + \int_1^R \lambda\left[C_n'(\xi) + \widetilde{\xi C_n''(\xi)} - \widetilde{\frac{\xi\gamma_E C_n(\xi)}{1+\alpha C_n(\xi)}}\right]d\xi \tag{A3}$$

Taking variation with respect to the independent variable C_n, we get

$$\delta C_{n+1}(R) = \delta C_n(R) + \delta\int_1^x \lambda\left[C_n'(\xi) + \widetilde{\xi C_n''(\xi)} - \widetilde{\frac{\xi\gamma_E C_n(\xi)}{1+\alpha C_n(\xi)}}\right]d\xi \tag{A4}$$

where λ is general Lagrangian multiplier, C_0 is initial approximation or trial function, $\widetilde{\xi C_n''(\xi)}$, $\widetilde{\frac{\xi\gamma_E C_n(\xi)}{1+\alpha C_n(\xi)}}$ and are considered as restricted

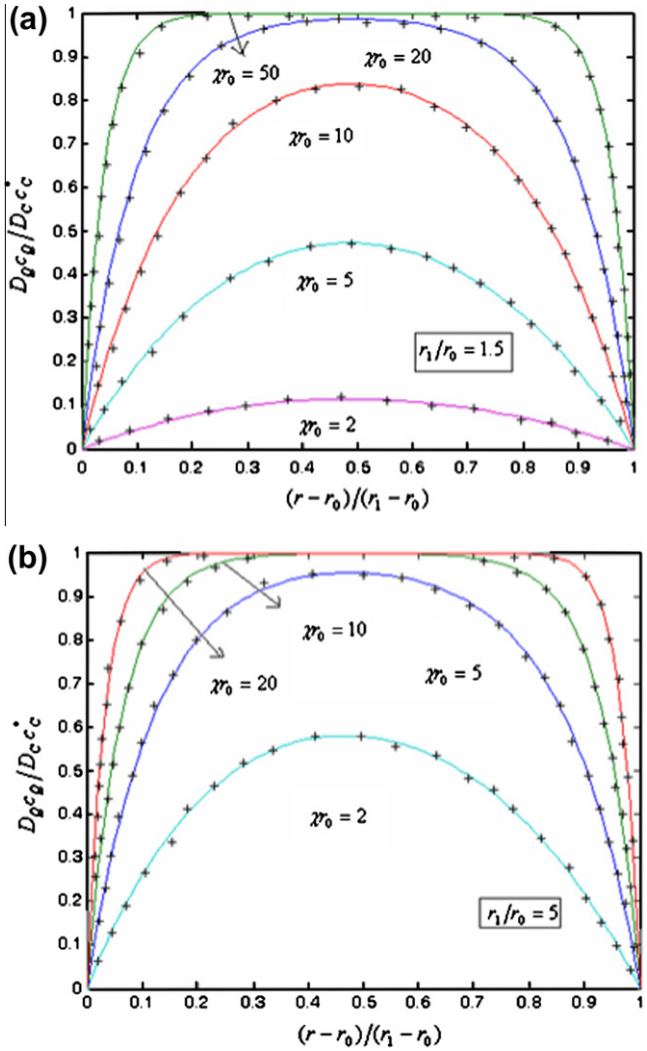

Fig. 6. Comparison of dimensionless steady-state concentration profile of *o*-quinone $D_Q c_Q(r)/D_C c_C^*$ with Rijiravanich et al. [17] results for various values of χr_0 and r_1/r_0. The key to the graph: (—) represents this work (Eq. (27)) and (+++) represents Rijiravanich et al. work (Eq. (31)).

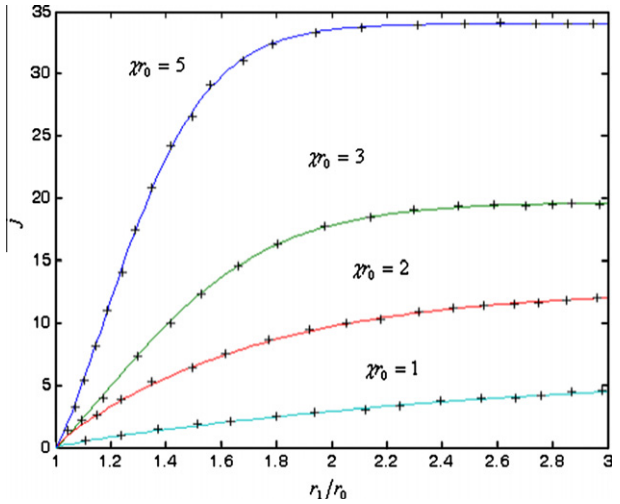

Fig. 7. Comparison of dimensionless steady-state sensor response *j* with Rijiravanich et al. [17] results for different enzyme reaction/substrate diffusion ratios χr_0. The key to the graph: (—) represents this work (Eq. (28)) and (+++) represents Rijiravanich et al. work (Eq. (32)).

variations, i.e. $\delta C_n'' = 0$ and $\frac{\delta C_n}{1+\alpha C_n} = 0$. Making the above correction functional (A4) stationary, noticing that $\delta C_n''(0) = 0$ and $\frac{\delta C_n(0)}{1+\alpha C_n(0)} = 0$.

$$\delta C_n : 1 + \lambda_1(\xi)|_{\xi=R} = 0 \tag{A5}$$

$$\delta C_n : -\lambda_1'(\xi)|_{\xi=R} = 0 \tag{A6}$$

The above equations are called Lagrange–Euler equations. By solving the above equations the Lagrange multiplier can be identified as

$$\lambda(\xi) = -1 \tag{A7}$$

Substituting the Lagrangian multiplier and $n = 0$ in the iteration formula (A3) we obtain,

$$(C_1(R) = C_0(R) - \int_1^R [C_0''(\xi) + \alpha C_0(\xi) C_0''(\xi) + (1/\xi) C_0'(\xi) + (\alpha C_0(\xi)/\xi) C_0'(\xi) - \gamma_E C_0(\xi)] d\xi \tag{A8}$$

Assuming that its initial approximate solution which satisfies the boundary conditions Eqs. (12) and (13) have the form

$$C_0(R) = [1 + a(1 - R^2)] \tag{A9}$$

By the iteration formula (A8) we have the (15) in the text.

Appendix B

Symbols used

Symbol	Definitions	Units
D_C	Diffusion coefficient of catechol	cm^2/s
c_C	Concentration profile of catechol	mole/cm^3
c_E	Concentration profile of enzyme	mole/cm^3
K_M	Michaelis Menten constant	mole/cm^3
K_{cat}	Catalytic rate constant	s^{-1}
c_Q	Concentration profile of quinone	mole/cm^3
D_Q	Diffusion coefficient of quinone	cm^2/s
c_C^*	Bulk concentration of *C*	mole/cm^3
r	Radius of the cylinder cm	
I	Current	Ampere
r_0	Electrode radius	cm
r_1	Film radius	cm
r_1/r_0	Dimensionless parameter for film thickness	none
χr_0	Dimensionless parameter for enzyme kinetic	none
j	Dimensionless sensor response	none
ψ	Dimensionless current	none
C	Dimensionless concentration of catechol	none
Q	Dimensionless concentration of quinone	none
R	Dimensionless distance	none
γ_E	Dimensionless reaction diffusion parameter	none
γ_S	Dimensionless reaction diffusion parameter	none
α	Dimensionless saturation parameter	none
L	Length of the electrode	cm
F	Faraday constant	c $mole^{-1}$
n	Number of electrons	none

References

[1] V. Desprez, P. Labbe, J. Electroanal. Chem. 415 (1996) 191.
[2] L. Coche-Guerente, V. Desprez, J.P. Diard, P. Labbe, J. Electroanal. Chem. 470 (1999) 53.
[3] L. Coche-Guerente, V. Desprez, P. Labbe, S. Therias, J. Electroanal. Chem. 470 (1999) 61.
[4] L. Coche-Guerente, P. Labbe, Virginie Mengeaud, Anal. Chem. 73 (2001) 3206.
[5] G. Decher, J.D. Hong, Ber. Bunsenges. Phys. Chem. 95 (1991) 1430.
[6] M. Onda, Y. Lvov, K. Ariga, T. Kunitake, Biotechnol. Bioeng. 51 (1996) 163.
[7] A.B. Garilov, A.F. Zueva, O.N. Efimov, V.A. Bogdanov-skaya, M.R. Tarasvitch, Synth. Mater. 60 (1993) 159.
[8] Y. Okahata, T. Tsuruta, K. Ijiro, K. Ariga, Thin Solid Films 180 (1989) 64.
[9] Hodak, R. Etchenique, E.J. Calbo, K. Singhal, P.N. Bartlett, Langmuir 13 (1997) 2708.
[10] Y. Lvov, K. Ariga, I. Ichinose, T. Kunitake, J. Am. Chem. Soc. 117 (1995) 6117.
[11] D. Laurent, J.B. Schelenoff, Langmuir 13 (1997) 1552.
[12] Y. Lvov, K. Ariga, I. Ichinose, T. Kunitake, Langmuir 12 (1996) 3038.
[13] G. Decher, Science 277 (1997) 1232.
[14] E.S. Forzani, V.M. Solis, E.S. Calvo, Anal. Chem. 72 (2000) 5300.
[15] A.S. Susha, F. Caruso, A.L. Rogach, G.B. Sukhorukov, A. Kornowski, H. Moewald, M. Giersig, A. Eychmueller, H. Weller, Colloids Surf. A 163 (2000) 39.
[16] F. Caruso, C. Schuler, Langmuir 16 (2000) 9595.
[17] P. Rijiravanich, K. Aoki, J. Chen, W. Surareungchai, M. Somasundrum, J. Electroanal. Chem. 589 (2006) 249.
[18] D.E. Wilcox, A.G. Porras, Y.T. Hwang, K. Lerch, M.E. Winkler, E.I. Solomon, J. Am. Chem. Soc. 107 (1985) 4015.
[19] J.H. He, Int. J. Nonlinear. Mech. 34 (4) (1999) 699.
[20] S. Momani, S. Abuasad, Chaos Solitons Fractals 27 (5) (2006) 1119.
[21] M.A. Abdou, A.A. Soliman, J. Comput. Appl. Math. 181 (2) (2005) 245.
[22] J.H. He, X.H. Wu, Chaos Solitons Fractals 29 (1) (2006) 108.
[23] L. Rajendran, G. Rahamathunissa, J. Math. Chem. 44 (2008) 49.
[24] D.D. Ganji, Seyed H. Hashemi Kachapi, Prog Nonlinear Sci. 2 (2011) 1.
[25] D.D. Ganji, Seyed H. Hashemi Kachapi, Prog Nonlinear Sci. 3 (2011) 1.
[26] J.H. He, G.C. Wu, Nonlinear Sci. Lett. A 1 (2010) 1.